

Elliptic flow splitting as a probe of the QCD phase structure at finite baryon chemical potential

Jun Xu,^{1,*} Taesoo Song,² Che Ming Ko,² and Feng Li²

¹*Shanghai Institute of Applied Physics, Chinese Academy of Sciences, Shanghai 201800, China*

²*Cyclotron Institute and Department of Physics and Astronomy,
Texas A&M University, College Station, Texas 77843, USA*

(Dated: April 18, 2019)

Using a partonic transport model based on the 3-flavor Nambu-Jona-Lasinio model and a relativistic hadronic transport model to describe, respectively, the evolution of the initial partonic and the final hadronic phase of heavy-ion collisions at energies carried out in the Beam-Energy Scan program at the Relativistic Heavy Ion Collider, we have studied the effects of both the partonic and hadronic mean-field potentials on the elliptic flow of particles relative to that of their antiparticles. We find that to reproduce the measured relative elliptic flow differences between nucleons and antinucleons as well as between kaons and antikaons requires a vector coupling constant as large as 0.5 to 1.1 times the scalar coupling constant in the Nambu-Jona-Lasinio model. Implications of our results in understanding the QCD phase structure at finite baryon chemical potential are discussed.

PACS numbers: 25.75.-q, 25.75.Ld, 25.75.Nq, 21.30.Fe, 24.10.Lx

The main purpose of the experiments involving collisions of heavy nuclei at relativistic energies is to study the properties of produced quark-gluon plasma (QGP) and its phase transition to hadrons. It is known from the lattice Quantum Chromodynamics (QCD) that for QGP of small baryon chemical potential, such as that formed at top energies of the Relativistic Heavy Ion Collider (RHIC) and the Large Hadron Collider (LHC), the hadron-quark phase transition (HQPT) is a smooth crossover [1, 2]. For QGP of finite baryon chemical potential produced at lower collision energies, studies based on various theoretical models have indicated, however, that the HQPT is expected to change to a first-order one [3–6]. To determine if the critical point, at which the crossover HQPT changes to a first-order one, exists and where it is located in the QCD phase diagram is important for understanding the phase structure of QCD and thus the nature of the strong interaction. To search for the critical point, the Beam-Energy Scan (BES) program has been carried out at RHIC to look for its signals at lower collision energies of $\sqrt{s_{NN}} = 7.7 \sim 39$ GeV.

Although there is no definitive conclusion on the existence or the location of the critical point, many interesting phenomena different from those at higher collision energies have been observed [7, 8]. Among them is the increasing splitting between the elliptic flow (v_2) of particles, i.e., the second Fourier coefficient in the azimuthal distribution of their momenta in the plane perpendicular to the participant or reaction plane, and that of their antiparticles with decreasing collision energy [9]. This result also indicates the breakdown of the number of constituent quark scaling of v_2 [10] at lower collision energies. The latter states that the scaled elliptic flow, which is obtained from dividing the hadron elliptic flow by its

number of constituent quarks as a function of a similarly scaled transverse kinetic energy, is similar for all hadrons, and this has been considered as an evidence for the existence of QGP in heavy-ion collisions at higher energies. Various explanations have been proposed to account for the observed splitting of particle and antiparticle v_2 . In Ref. [11], it was suggested that in the presence of the strong magnetic field in non-central heavy-ion collisions, the chiral magnetic wave induced by the axial anomaly in QCD can generate an electric quadrupole moment in the produced baryon-rich QGP. This can then lead to the splitting of the v_2 of oppositely charged particles and antiparticles, particularly that of π^+ and π^- due to their similar final-state interactions in the hadronic matter. The v_2 splitting of particles and antiparticles may also be attributed to different v_2 of transported and produced partons [12], different rapidity distributions of quarks and antiquarks [13], and the conservation of baryon charge, strangeness, and isospin [14].

On the other hand, we have shown in our previous studies that the different mean-field potentials for hadrons and antihadrons [15] or quarks and antiquarks [16] in the baryon-rich matter produced at lower collision energies can describe qualitatively the v_2 splitting of particles and their antiparticles. This is due to the fact that particles with attractive potentials are more likely to be trapped in the system and move in the direction perpendicular to the participant plane, while those with repulsive potentials are more likely to leave the system and move along the participant plane, thus reducing and enhancing their respective elliptic flows. However, the relative v_2 difference between p and \bar{p} was underestimated in both our previous studies, and that between K^+ and K^- was overestimated in Ref. [15] with only hadronic potentials and underestimated in Ref. [16] with only partonic potentials.

In the present study, we include both the partonic potentials from the Nambu-Jona-Lasinio (NJL) model [17]

*Electronic address: xujun@sinap.ac.cn

and the hadronic potentials that were known in the literature on subthreshold particle production in heavy-ion collisions [18, 19]. To reproduce quantitatively the relative v_2 difference for p and \bar{p} as well as K^+ and K^- in mini-bias Au+Au collisions at $\sqrt{s_{NN}} = 7.7$ GeV, we find that the ratio R_V of the vector coupling G_V to the scalar-pseudoscalar coupling G in the NJL model is constrained to values between 0.5 and 1.1. It has been shown that this ratio determines the density beyond which the quark matter is formed in hybrid stars [20], which is important in understanding the composition of the recently discovered two-solar-mass neutron star [21]. More importantly, studies based on both the NJL model and the Polyakov-Nambu-Jona-Lasinio (PNJL) model [3–6] have shown that the existence and the location of the HQPT critical point in the QCD phase diagram depends on the value of R_V . Our results thus suggest that studying the v_2 splitting of particles and their antiparticles provides the possibility of mapping out the QCD phase diagram at finite baryon chemical potential and to better understand the nature of the strong interaction.

We include the mean-field potential effect by extending the string-melting version of a multiphase transport (AMPT) model [22], which has been successfully used to describe the harmonic flows and the di-hadron correlation at both RHIC and LHC [23]. In this model, the initial hadrons, which are generated by the Heavy-Ion Jet Interaction Generator (HIJING) model [24] via the Lund string fragmentation model, are converted to their constituent or valence quarks and antiquarks. Different from previous studies at higher energies, the evolution of partons in time and space is modeled by a 3-flavor NJL transport model [16]. The NJL Lagrangian is written as [6]

$$\begin{aligned} \mathcal{L} = & \bar{\psi}(i \not{\partial} - M)\psi + \frac{G}{2} \sum_{a=0}^8 \left[(\bar{\psi}\lambda^a\psi)^2 + (\bar{\psi}i\gamma_5\lambda^a\psi)^2 \right] \\ & + \sum_{a=0}^8 \left[\frac{G_V}{2} (\bar{\psi}\gamma_\mu\lambda^a\psi)^2 + \frac{G_A}{2} (\bar{\psi}\gamma_\mu\gamma_5\lambda^a\psi)^2 \right] \\ & - K \left[\det_f \left(\bar{\psi}(1 + \gamma_5)\psi \right) + \det_f \left(\bar{\psi}(1 - \gamma_5)\psi \right) \right], \quad (1) \end{aligned}$$

with the quark field $\psi = (\psi_u, \psi_d, \psi_s)^T$, the current quark mass matrix $M = \text{diag}(m_u, m_d, m_s)$, and the Gell-Mann matrices λ^a in $SU(3)$ flavor space. In the case that the vector and axial-vector interactions are generated by the Fierz transformation of the scalar and pseudo-scalar interactions, their coupling strengths are given by $G_V = G_A = G/2$, while $G_V = 1.1G$ was used in Ref. [25] to give a better description of the vector meson-mass spectrum based on the NJL model. Other parameters are taken from Refs. [6, 25] as $m_u = m_d = 3.6$ MeV, $m_s = 87$ MeV, $G\Lambda^2 = 3.6$, $K\Lambda^5 = 8.9$, and $\Lambda = 750$ MeV is the cut-off value in the momentum integration. In the mean-field approximation, the above Lagrangian leads to an attractive scalar mean-field potential for both quarks and antiquarks [16]. With a nonvanishing G_V , it

further gives rise to a repulsive vector mean-field potential for quarks but an attractive one for antiquarks in a baryon-rich quark matter.

For the scattering cross sections between quarks and antiquarks, we assume that they are isotropic and have a constant value that is determined from fitting the measured charged-particle elliptic flow. The quark matter then evolves under the influence of both mean-field potentials and two-body scatterings until the chiral symmetry is broken, i.e., the effective mass of light quarks, which is determined by Eq. (4) in Ref. [16], is larger than about 200 MeV.

At hadronization, quarks and antiquarks in the AMPT model are converted to hadrons via a spatial coalescence model, and the scatterings between hadrons in the hadronic stage are described by a relativistic transport (ART) model [26] that has been extended to also include particle-antiparticle annihilations and their inverse reactions. For the hadronic potentials, they are included as in our previous work [15] using the phenomenologically determined relativistic mean-field model [18] for nucleons and antinucleons, and effective chiral Lagrangian [19] for kaons and antikaons. Due to the G-parity invariance, the potential for antinucleons is much more attractive than that for nucleons, and that for kaons is slightly repulsive while that for antikaons is deeply attractive in a baryon-rich hadronic matter.

For the centrality of heavy-ion collisions, we use the empirical formula $c = \pi b^2/\sigma_{in}$ [27] to determine the relation between the centrality c used in the experimental analysis and the impact parameter b , where the total nucleus-nucleus inelastic cross section is $\sigma_{in} \approx 686$ fm² from the Glauber model calculation using the nucleon-nucleon inelastic cross section of about 30.8 mb at $\sqrt{s_{NN}} = 7.7$ GeV from Ref. [28]. The mean-field potentials in both the partonic phase and the hadronic phase are then calculated using the test particle method [29] with parallel events that correspond to the same impact parameter.

To fix the parton scattering cross section in the NJL transport model, we compare the transverse momentum (p_T) dependence of the elliptic flow of mid-pseudorapidity charged particles measured in mid-central Au+Au collisions at $\sqrt{s_{NN}} = 7.7$ GeV with results obtained for different values of the parton scattering cross section σ . The elliptic flow is calculated from the average azimuthal anisotropy of particles with respect to the participant plane, i.e., $v_2 = \langle \cos[2(\phi - \Psi_2)] \rangle$, where $\phi = \text{atan2}(p_y, p_x)$ is the azimuthal angle of the particle momentum at the final stage, and $\Psi_2 = [\text{atan2}(\langle r_p^2 \sin 2\phi_p \rangle, \langle r_p^2 \cos 2\phi_p \rangle) + \pi]/2$ is the azimuthal angle of the participant plane at the initial stage with r_p and ϕ_p being the polar coordinates of the participants. As shown in Fig. 1, the v_2 of charged hadrons is larger for a larger parton scattering cross section, and we find that the experimentally measured v_2 of charged particles from the STAR Collaboration [28] can be reasonably reproduced with a parton scattering cross sec-

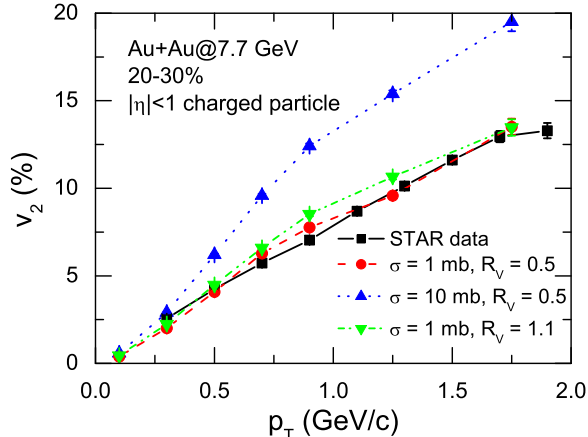


FIG. 1: (Color online) Transverse momentum dependence of the elliptic flow of mid-pseudorapidity charged particles in mid-central Au+Au collisions at $\sqrt{s_{NN}} = 7.7$ GeV for different values of the parton scattering cross section σ and the ratio R_V of the vector coupling constant G_V to the scalar coupling constant G in the NJL model. The experimental data from the STAR Collaboration is from Ref. [28].

tion of $\sigma = 1$ mb. This value is about half the average of quark-quark and quark-antiquark elastic cross sections calculated from the NJL model [30]. The magnitude of v_2 is, however, rather insensitive to the value of R_V , as increasing R_V from 0.5 to 1.1 only increases slightly the value of v_2 . These results remain similar if different methods are used to calculate the hadron v_2 .

Figure 2 displays the p_T dependence of v_2 for mid-pseudorapidity nucleons and kaons as well as their antiparticles right after hadronization in mini-bias Au+Au collisions at $\sqrt{s_{NN}} = 7.7$ GeV, with the parton scattering cross section of 1 mb as determined above. Due to the different mean-field potentials for quarks and antiquarks in the baryon-rich quark matter, the v_2 for nucleons and K^- formed from the spatial coalescence of partons are larger than that for antinucleons and K^+ , respectively. In addition, the v_2 splitting is larger with a larger value of R_V , especially for nucleons and antinucleons. These results are qualitatively consistent with those in Ref. [16] although different parton scattering cross sections and hadronization criteria are used.

The final differential elliptic flows after the evolution of the hadronic phase are shown in Fig. 3, and they are larger than their corresponding values in the beginning of the hadronic stage. Because of the repulsive potential for nucleons and the attractive potential for antinucleons in the baryon-rich hadronic matter, the v_2 of nucleons, which is larger initially, remains larger than that of antinucleons after hadronic evolution. For the v_2 of K^+ and K^- , which is initially larger for K^- than for K^+ , the ordering is, on the other hand, reversed by the repul-

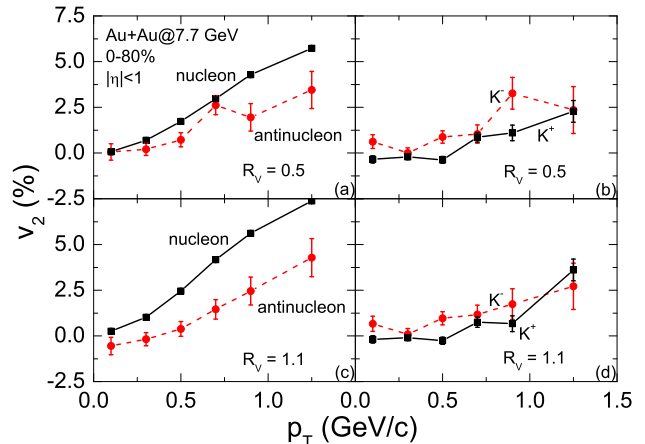


FIG. 2: (Color online) Transverse momentum dependence of the elliptic flows of mid-pseudorapidity nucleons and kaons as well as their antiparticles right after hadronization in mini-bias Au+Au collisions at $\sqrt{s_{NN}} = 7.7$ GeV for different values of $R_V = G_V/G$ in the NJL model.

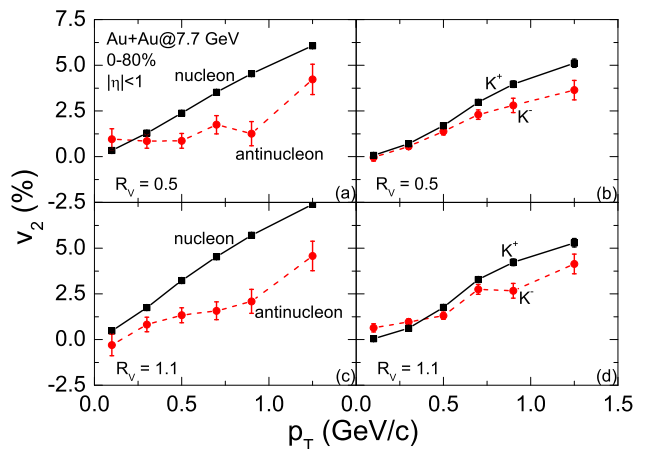


FIG. 3: (Color online) Same as Fig. 2 but for results after hadronic evolution.

sive K^+ and attractive K^- potential in the baryon-rich hadronic matter, resulting in a larger v_2 for K^+ than for K^- after hadronic evolution. These effects are seen for both values of R_V .

Figure 4 compares the p_T -integrated relative elliptic flow differences $[v_2(P) - v_2(\bar{P})]/v_2(P)$ between nucleons and antinucleons as well as between kaons and antikaons for different values of R_V with the experimental results from the STAR Collaboration [8]. The STAR results can now be quantitatively reproduced with both $R_V = 0.5$ and $R_V = 1.1$ within the statistical error. Also, we find that with increasing value of R_V the relative v_2 differ-

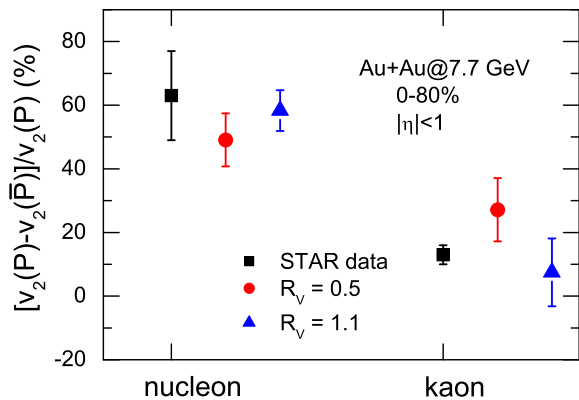


FIG. 4: (Color online) Relative elliptic flow difference between nucleons and antinucleons as well as kaons and antikaons for different values of $R_V = G_V/G$ in the NJL model compared with the STAR data [8].

ence between nucleons and antinucleons increases, while that between kaons and antikaons decreases, consistent with the results in Ref. [16]. It is thus expected that further reducing the value of R_V would underestimate the relative v_2 difference between nucleons and antinucleons and overestimate that between kaons and antikaons, while further increasing the value of R_V would underestimate that between kaons and antikaons. To reproduce both the relative v_2 differences for nucleons and antinucleons as well as that for kaons and antikaons requires the value of R_V to be within 0.5 and 1.1. According to Refs. [3–6], such values of vector coupling would make the critical point disappear in the QCD phase diagram, and the hadron-quark phase transition would always be a smooth crossover. Furthermore, a larger value of R_V

results in a hadron-quark phase transition at very high densities or even a disappearance of the quark phase in neutron stars [20], leading to a possible explanation for the observed two-solar-mass neutron star [21].

In summary, we have studied the effects of both the partonic and the hadronic potential on the elliptic flow splitting of particles and their antiparticles in relativistic heavy-ion collisions carried out in the BES program at RHIC. With the evolution of the partonic phase described by an NJL transport model, we have obtained a larger v_2 for nucleons and K^- than antinucleons and K^+ , respectively, right after hadronization. After the hadronic evolution described by a relativistic transport model that includes the empirically determined hadronic potentials for particles and antiparticles, the final v_2 is larger for nucleons and K^+ than antinucleons and K^- , respectively. The relative v_2 differences from the STAR data can be reproduced if the ratio R_V of the vector coupling constant G_V to the scalar coupling constant G in the NJL model is between 0.5 and 1.1, after taking into account the mean-field potential effects in both the partonic and the hadronic phase. Our results therefore suggest that studying the v_2 splitting of particles and their antiparticles in heavy-ion collisions provides the possibility of studying the QCD phase structure at finite baryon chemical potential, thus helping understand the nature of the strong interaction.

Acknowledgments

One of us (Jun Xu) would like to thank Zi-Wei Lin for helpful communications. This work was supported by the “100-talent plan” of Shanghai Institute of Applied Physics under grant Y290061011 from the Chinese Academy of Sciences, the US National Science Foundation under Grant No. PHY-1068572, and the Welch Foundation under Grant No. A-1358.

-
- [1] C. Bernard *et al.* (MILC Collaboration), Phys. Rev. D **71**, 034504 (2005).
 - [2] A. Bazavov *et al.*, Phys. Rev. D **85**, 054503 (2012).
 - [3] M. Asakawa and K. Yazaki, Nucl. Phys. **A504**, 668 (1989).
 - [4] K. Fukushima, Phys. Rev. D **77**, 114028 (2008) [Erratum-ibid. D **78**, 039902 (2008)].
 - [5] S. Carignano, D. Nickel, and M. Buballa, Phys. Rev. D **82**, 054009 (2010).
 - [6] N. M. Bratovic, T. Hatsuda, and W. Weise, arXiv: 1204.3788 [hep-ph].
 - [7] L. Kumar (STAR Collaboration), J. Phys. G **38**, 124145 (2011).
 - [8] B. Mohanty (STAR Collaboration), J. Phys. G **38**, 124023 (2011).
 - [9] L. Adamczyk *et al.* (STAR Collaboration), Phys. Rev. Lett. **110**, 142301 (2013).
 - [10] A. Adare *et al.* (STAR Collaboration), Phys. Rev. Lett. **98**, 162301 (2007).
 - [11] Y. Burnier *et al.*, Phys. Rev. Lett. **107**, 052303 (2011).
 - [12] J. C. Dunlop, M. A. Lisa, and P. Sorensen, Phys. Rev. C **84**, 044914 (2011).
 - [13] V. Greco, M. Mitrovski, and G. Torrieri, Phys. Rev. C **86**, 044905 (2012).
 - [14] J. Steinheimer, V. Koch, and M. Bleicher, Phys. Rev. C **86**, 044903 (2012).
 - [15] J. Xu, L. W. Chen, C. M. Ko, and Z. W. Lin, Phys. Rev. C **85**, 041901 (2012).
 - [16] T. Song, S. Plumari, V. Greco, C. M. Ko, and F. Li, arXiv:1211.5511 [nucl-th].
 - [17] Y. Nambu and G. Jona-Lasinio, Phys. Rev. **122**, 345 (1961); **124**, 246 (1961).
 - [18] G. Q. Li *et al.*, Phys. Rev. C **49**, 1139 (1994).
 - [19] G. Q. Li *et al.*, Nucl. Phys. **A625**, 372 (1997).

- [20] G. Y. Shao *et al.*, arXiv: 1305.1176 [nucl-th].
- [21] P. B. Demorest *et al.*, *Nature* **467**, 1081 (2010).
- [22] Z. W. Lin *et al.*, *Phys. Rev. C* **72**, 064901 (2005).
- [23] J. Xu and C. M. Ko, *Phys. Rev.* **83**, 021903 (R) (2011); **83**, 034904 (2011); **84**, 014903 (2011); **84**, 044907 (2011).
- [24] X. N. Wang and M. Gyulassy, *Phys. Rev. D* **44**, 3501 (1991).
- [25] M. F. M. Lutz, S. Klimt, and W. Weise, *Nucl. Phys.* **A542**, 521 (1992).
- [26] B. A. Li and C. M. Ko, *Phys. Rev. C* **52**, 2037 (1995).
- [27] W. Broniowski and W. Florkowski, *Phys. Rev. C* **65**, 024905 (2002).
- [28] L. Adamczyk *et al.* (STAR Collaboration), *Phys. Rev. C* **86**, 054908 (2012).
- [29] C. Y. Wong, *Phys. Rev. C* **25**, 1460 (1982).
- [30] R. Marty, E. Bratkovskaya, W. Cassing, J. Aichelin, and H. Berrehrak, arXiv:1305.7180 [hep-ph].